CONF-950336--29

CONDENSATION OF REFRIGERANTS FLOWING INSIDE SMOOTH AND CORRUGATED TUBES

Darrell L. Hinton
Tennessee State University
Nashville, Tennessee

James C. Conklin
Edward A. Vineyard
Oak Ridge National Laboratory
Oak Ridge, Tennessee

To be presented at the
4th ASME/JSME
Thermal Engineering Joint Conference
Maui, Hawaii
March 19-24, 1995

Research sponsored by the Office of Building Technologies, U.S. Department of Energy under contract No. DE-AC05-84OR21400 with Oak Ridge National Laboratory, managed by Martin Marietta Energy Systems, Inc.

CONDENSATION OF REFRIGERANTS FLOWING INSIDE SMOOTH AND CORRUGATED TUBES

Darrell L. Hinton
Tennessee State University
Nashville, Tennessee

James C. Conklin
Edward A. Vineyard
Oak Ridge National Laboratory
Oak Ridge, Tennessee

ABSTRACT

Because heat exchanger thermal performance has a direct influence on the overall cycle performance of vapor-compression refrigeration machinery, enhanced heat transfer surfaces are of interest to improve the efficiency of heat pumps and air conditioners. We investigated R-22 and a nonazeotropic refrigerant mixture (NARM) of 75% R-143a and 25% R-124 (by mass) to study their thermal performance in a condenser made of conventional smooth tubes and another condenser made of corrugated, or spirally indented, tubes.

We investigated the condensing heat transfer and pressure drop characteristics in an experimental test loop model of a domestic heat pump system employing a variable speed compressor. The refrigerant circulates inside the central tube and the water circulates in the annulus. At refrigerant mass fluxes of approximately 275–300 kg/m^{2}s, the measured irreversible pressure drop of the corrugated surface was 23% higher than that of the smooth surface for the R-22. At refrigerant mass fluxes of 350–370 kg/m^{2}s, the irreversible pressure drop of the corrugated surface was 36% higher than that of the smooth surface for the NARM. The average heat transfer coefficient for the corrugated surface for R-22 was roughly 40% higher than that for the smooth tube surface at refrigerant mass fluxes of 275–295 kg/m^{2}s. The average heat transfer coefficient for the corrugated surface for the NARM was typically 70% higher than that for the smooth tube surface at refrigerant mass fluxes of 340–385 kg/m^{2}s.

NOMENCLATURE

A	Area, heat transfer (m^2)
c	Specific heat at constant pressure (J·kg^{-1}·K^{-1})
d	Diameter (m)
e	Spiral indentation depth (m)
h	Heat transfer coefficient (W·m^{-2}·K^{-1})
k	Thermal conductivity (W·m^{-1}·K^{-1})
l	Length (m)
$\dot{m}$	Mass flow rate (kg·s^{-1})
q''	Heat flux (W·m^{-2})
T	Temperature (K)
ΔT	Temperature difference (K)
U	Overall heat transfer coefficient (W·m^{-2}·K^{-1})

Subscripts

cu	copper
hyd	hydraulic
i	inlet
l	liquid
lm	log mean
o	outlet
r	refrigerant
w	water

Dimensionless Quantities

Pr	Prandtl number
Re	Reynolds number

INTRODUCTION

Augmented heat exchanger surfaces are being studied to improve the efficiency of heat pumps. Researchers are investigating nonazeotropic refrigerant mixtures (NARMs) as replacements for the chlorofluorocarbon (CFC) refrigerants presently used in refrigeration equipment. For NARMs in the wet (two-phase) region, the saturation temperature at constant pressure varies with respect to quality; thus, the condensation process is not isothermal. The thermodynamic cycle efficiency can be improved by bringing the mean refrigerant temperature closer to the process fluid inlet temperature (Rice, 1993). This nonisothermal phase-change behavior implies that a specific heat exists in the two-phase region. Furthermore, many refrigerant mixtures have non-linear temperature-enthalpy relationships in the two-phase region which implies a varying specific heat (Granryd and Conklin, 1990). This report presents the NARM condensation heat transfer coefficient inside a smooth and an enhanced corrugated tube surface. To establish a series of base conditions, this report also presents the R-22 condensing heat transfer inside a smooth and a corrugated tube surface.

We chose the non-CFC refrigerants R-143a and R-124 for testing based on a previous research effort (Vineyard et al., 1989) which screened refrigerant pairs using such factors as boiling point, stability, ozone depletion potential and coefficient of performance to determine suitable candidates for residential heat pump operation. We selected a mixture of 75% R-143a and 25% R-124 (by mass) for condensation at various mass flow rates. Because we used water-to-refrigerant heat exchangers in the experimental apparatus, we selected inlet water temperatures that would yield R-22 saturation pressures equivalent to those determined for air-to-refrigerant heat exchangers by the U.S. Department of Energy (DOE) standard rating conditions for heat pumps (Miller, 1989). The water temperature change was chosen to match typical air-to-refrigerant temperature differences.

EXPERIMENTAL APPARATUS

We investigated the heat transfer from enhanced surfaces during tubeside condensation of R-22 and the NARM by using the instrumented apparatus, shown in Fig. 1, that consists of a variable-speed compressor having a range of 500–3000 rpm that allows for variable heat exchanger loadings; a variable orifice refrigerant metering device (needle valve); and two sets of counterflow concentric tube heat exchangers that have two different tubeside surfaces. The refrigerant circulates inside the central tube and the water circulates in the annulus. We chose a variable-speed compressor to provide for different heat loadings of the

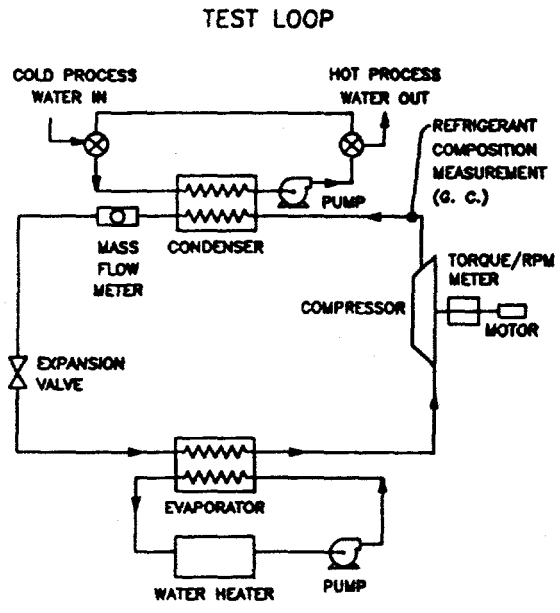

FIGURE 1.
NONAZEOTROPIC REFRIGERANT MIXTURE TEST LOOP.

heat exchangers. We decided on a needle valve for flexibility in controlling refrigerant conditions, because this flexibility is lacking in capillary tubes and thermal expansion valves.

The heat exchangers, with instrumentation as shown in Fig. 2, consist of a central tube and an outer tube forming an annulus. Care was taken during assembly to insure a concentric annulus. There are eight horizontal passes where the outer surfaces of the water annulus and the refrigerant bends are insulated. The smooth surface tube is copper and has an outer diameter of 18.923 mm and an inner diameter of 16.789 mm. Each cooled horizontal section is 1.94 m in length.

The corrugated surface tube, as shown in Fig. 3, is also copper and has an outer diameter (d_o) of 15.788 mm and an inner diameter (d_i) of 13.656 mm. The spiral indentations are approximately 0.8 mm in depth (e), having two indentations at a given cross-section and a pitch (i.e., axial distance between two indentations p) of 7.1 mm. This pitch results in a helix angle of approximately 80° with respect to the longitudinal axis of the tube. Each cooled horizontal section is 1.94 m in length. We attribute the differences in the dimensions of the smooth and corrugated tubes to commercial availability.

TESTING PROCEDURE

The system was evacuated to a hard vacuum and then liquid charged with the refrigerant mixture. In addition, we

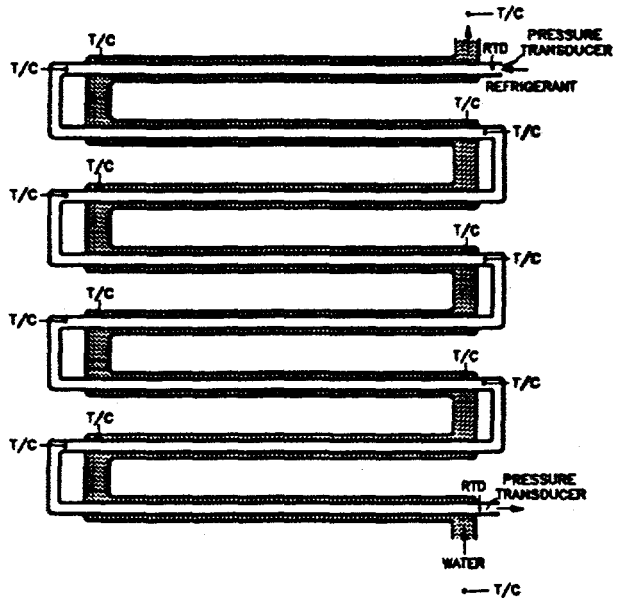

FIGURE 2. HEAT EXCHANGER SCHEMATIC DIAGRAM.

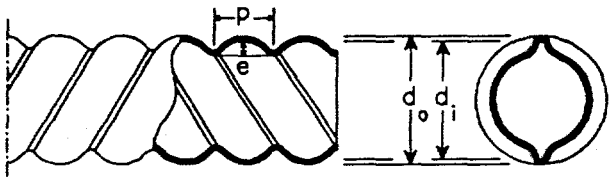

FIGURE 3. CORRUGATED TUBE GEOMETRY.

used a dedicated gas chromatograph (G. C.), located at the compressor exit, to monitor the composition of the circulating charge in real time. We recorded the output of instrumentation such as mass flowmeters, pressure transducers, thermocouples, and resistance temperature devices (RTDs) as shown in Figs. 1 and 2 on a minicomputer, taking data every fifteen seconds averaged over a fifteen minute period during steady-state operation. All pressure transducers, flowmeters, thermocouples, and RTDs were calibrated prior to testing.

We controlled water flow rates to the heat exchangers to allow for rapid changes in test conditions. We maintained inlet temperatures to the condenser with a mixing valve that introduces cool process water while bleeding off warmer water that has passed through the condenser. We controlled inlet water temperatures to the evaporator by using a bank of resistance heaters in the closed-loop system.

We based test conditions on DOE standard cooling rating condition for an air-source heat pump. We adjusted inlet water temperatures to yield R-22 saturation pressures equivalent to those determined from previous testing with an air-source system (Miller, 1989). For this system, the R-22 condenser inlet pressure was approximately 1500 kPa. We determined the heat rates for the refrigerant side and the water side for both heating and cooling modes from measured inlet and outlet temperatures and measured flow rates and then checked for a steady-state heat balance. A test was acceptable when the heat rates agreed to within 5%. We also used the electrical power measurements for the closed loop system to check for a heat balance in steady-state operation. We determined the needed refrigerant thermodynamic properties from algorithms presented by Morrison and McLinden (1986) that implement the Carnahan-Starling-DeSantis equation of state.

During the testing, we maintained minimal subcooling (to within 5°C) at the condenser exit and minimal superheating (to within 5°C) at the evaporator exit to ensure two-phase conditions in the heat exchangers. The mass flows of the NARM were varied to meet comparable cooling capacities for R-22, hence, the mass fluxes for the NARM and R-22 are different for the same evaporator loadings.

The R-22 and the NARM had an alkylbenzene oil present for lubrication of the compressor. The concentration of oil, which we did not monitor during the tests, was on the order of 1%. We did not investigate the effect of oil on the heat transfer coefficient or pressure drop. The effect of lubricants may be substantial (Schlager et al., 1990), but we did not consider it because of system instrumentation limitations. Hence, this report compares the performance of two refrigerants, one pure and the other a mixture, condensing from two different surfaces under equivalent conditions with approximately 1% lubricant.

HEAT TRANSFER ANALYSIS

To assess the thermal performance of the corrugated and the smooth tubes, as used here for condensation, the measured average smooth tube heat transfer coefficient was compared with the measured average corrugated tube heat transfer coefficient. Any augmentation effects of the corrugated tube with respect to the smooth tube should be identified by this presentation.

Because one objective of this study was to measure the thermal performance of R-22 and the NARM in the

condenser, we computed a condensing heat transfer coefficient from the measured temperatures and flows. First, we computed a "standard" log mean temperature difference from the measured condenser inlet and outlet temperatures of the two-phase region with the following equation:

$$\Delta T_{lm} = \frac{(T_{w,i} - T_{r,o}) - (T_{w,o} - T_{r,i})}{\ln\left(\frac{T_{w,i} - T_{r,o}}{T_{w,o} - T_{r,i}}\right)} , \quad (1)$$

where T represents a temperature. Subscript r represents the refrigerant, w represents the water, i represents the corresponding flow inlet, and o represents the corresponding flow outlet.

The average heat flux from the refrigerant during the condensation process was then determined from the measured water temperatures and flow rate with the following equation:

$$q'' = \frac{\dot{m}_w c_w (T_{w,i} - T_{w,o})}{A_w} , \quad (2)$$

where A_w represents the heat transfer area of the outer surface of the refrigerant tube to the water. The outer annulus was insulated and an estimate of the radial heat loss through the outer insulation showed that no more than 0.1% of the heat transferred by the water was transferred by natural convection to the ambient conditions of the laboratory. Thus, we ignored heat gains from the environment.

We then determined an overall heat transfer coefficient as follows:

$$U = \frac{q''}{\Delta T_{lm}} . \quad (3)$$

Axial heat losses along the copper tube were ignored in Eq. (2). To justify this assumption, we computed the ratio of the convection conductance ($U \cdot A_w$) and the axial thermal conductance ($k_{cu} \cdot A_{cu}/l$). This ratio was on the order of 3×10^4, indicating a much greater resistance to the flow of heat along the tube wall as compared with the flow of heat convected to the fluids through the tube wall. Thus, only radial heat transfer was used for computing the overall heat transfer coefficient.

Representing the Prandtl number of the water by Pr_w and representing the Reynolds number of the flow based on the hydraulic diameter of the annulus by Re_w, we obtained the heat transfer coefficient to the water from the following empirical relationship:

$$h_w = \frac{k_w}{d_{hyd}} a Re_w^{0.8} Pr_w^{0.4} . \quad (4)$$

The coefficient a, equal to 0.0164 for the smooth tube annulus and 0.0406 for the corrugated tube annulus used in this study, and the exponent of the Reynolds number were obtained using a modified Wilson plot method that Shah (1990) attributes to Briggs and Young (1969), using test data we obtained with R-22. We ignored viscosity variations because the difference in temperature between the tube wall and the water was less than 10°C.

The heat transfer coefficient of the refrigerant was then computed by the following equation:

$$h_r = \frac{1}{\frac{A_r}{A_w}\left(\frac{1}{U} - \frac{1}{h_w}\right)} , \quad (5)$$

where A_r represents the heat transfer area of the inner tube surface to the refrigerant. The flow area and heat transfer area of the corrugated surface are those of the equivalent unenhanced surface—any fin effect of the indentations is thus considered only implicitly. The equivalent unenhanced surface is that due to the undimpled diameter, given as d_i in Fig. 3. Because the tubes are copper, the thermal resistance of the tube material was neglected. Because the tubes were new, no fouling factor was assigned and no fouling was observed upon visual inspection subsequent to testing.

The heat transfer coefficient reported here is an average, or a mean value over five tube lengths that we observed to be in the two-phase region as shown in subsequent figures. The reported heat transfer coefficient is not a mean value for the entire length of the heat exchanger. The quality range of the refrigerant was approximately 10%–90%. During this quality change, a change in temperature occurs, thus a specific heat in this two-phase region can be defined (Granryd and Conklin, 1990). Equation (1), which computes the log-mean temperature difference, has a limiting assumption of a constant specific heat of the refrigerant. This assumption may not be valid over the range of pressures and temperatures experienced in the tests for evaluating the mean condensing heat transfer coefficient of this NARM (Granryd and Conklin, 1990). For the scoping purposes of this investigation to observe heat transfer augmentation of the corrugated surface, however, the error committed for the NARM should be approximately the same for the corrugated and smooth

surfaces. Use of the arithmetic mean refrigerant temperature is less accurate than the log mean temperature difference (Rice, 1993). Where needed, we determined the refrigerant thermodynamic properties from algorithms presented by Morrison and McLinden (1986) that implement the Carnahan-Starling-DeSantis equation of state.

HEAT TRANSFER RESULTS AND DISCUSSION

The mean heat transfer coefficient computed with Eq. (5) has an approximate uncertainty of 20%. We computed this uncertainty from a propagation of error analysis (Box et al., 1978) that included the uncertainties of 0.28°C for the thermocouples and 3% of measured flow for the flowmeter. This uncertainty does not include the possible error introduced by the varying specific heat of the NARM in the two-phase region.

Figure 4 illustrates the variation in the average heat transfer coefficient with respect to mass flux for R-22 and the NARM in both smooth and corrugated tube geometries. As may be observed in the figure, the condensing coefficient increases with increasing mass flux as is consistent with results found by other researchers. The heat transfer coefficient of the NARM is consistently lower than that of R-22. For the smooth tube, the heat transfer coefficient for R-22 being typically 60% higher than that of the NARM for refrigerant mass fluxes of 225–280 kg/m^{2}s. For the corrugated tube, the heat transfer coefficient for R-22 is on the average 20% higher than that for the NARM for refrigerant mass fluxes of 345–390 kg/m^{2}s. Two possible explanations for the significantly lower heat transfer of the NARM in the smooth tube are a mass diffusion resistance in the liquid phase and a variation of thermophysical properties of the two constituent refrigerants. Other heat transfer degradation mechanisms may also exist. Note that the heat transfer coefficient is only 20% lower in the corrugated tube as compared to 60% lower in the smooth tube geometry. Hence, the corrugated tube geometry is apparently mitigating the NARM heat transfer degradation mechanisms, perhaps by increased mixing.

Figures 5 and 6 present temperature profiles of the water and refrigerant for R-22 and the NARM respectfully versus condenser length for the smooth tube condenser. Similarly, Figures 7 and 8 present the temperature profiles in the corrugated geometry. The refrigerant inlet is at zero meters and the water inlet is at 15.2 meters. The temperature profiles are for the entire condenser length, although only tube passes 2–7 (from positions 2 m to 13 m on the plots) were utilized in calculating the average heat transfer coefficient. These temperature profiles are presented to indicated the two-phase region in the condenser and also to

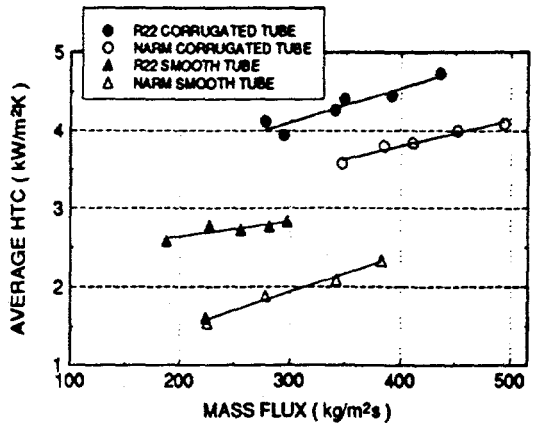

FIGURE 4. AVERAGE MEASURED HTC FOR SMOOTH AND CORRUGATED TUBE CONDENSERS.

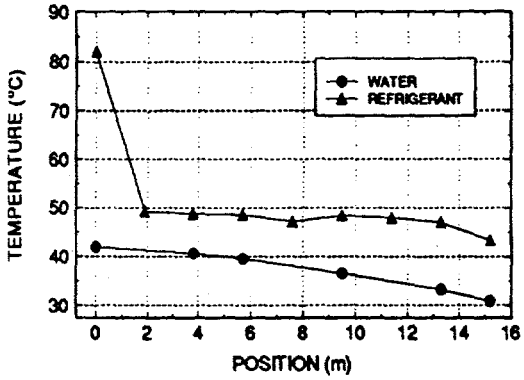

FIGURE 5. R-22 FLOWING INSIDE SMOOTH TUBE AT MASS FLUX = 281 kg/m^{2}s.

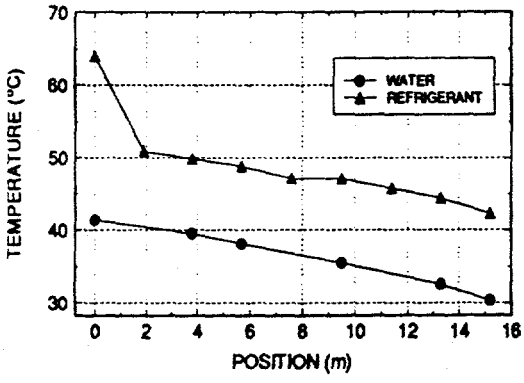

FIGURE 6. NARM FLOWING INSIDE SMOOTH TUBE AT MASS FLUX = 278 kg/m^{2}s .

indicate an inherent advantage of NARMs—the temperature glide that can lead to increased cycle efficiency (Vineyard et al., 1993).

For the smooth tube, Figure 5 shows that the refrigerant temperature is essentially constant in the two phase region (4 – 13 meters) for R-22, any deviation being attributed to pressure variation along the condenser, whereas in Figure 6 a temperature decrease of approximately 7°C occurs in the phase change region for the NARM. Similarly, Figures 7 and 8 for the corrugated tube show the same behavior, but at a decreased temperature difference between the refrigerant and the water, reflecting the increased thermal performance of the corrugated surface for heat transfer.

Pressure drop. The static pressure drop is measured from the superheated vapor inlet to the subcooled liquid outlet. The reversible pressure recovery due to condensation is then subtracted—the irreversible pressure drops for the smooth and corrugated tube condensers vs. mass flux are presented in Fig. 9. This irreversible pressure drop is reported here because of the scoping nature of this study to compare smooth and roughened surfaces using pure and mixed refrigerants. Not surprisingly, the pressure drop for the corrugated tube is everywhere higher than that for the smooth tube for both R-22 and the NARM at any given mass flux. At refrigerant mass fluxes of 275 to 300 kg/m^{2}s, the irreversible pressure drop for the corrugated surface is 23% higher than that for the smooth surface for R-22. At refrigerant mass fluxes of 350 to 370 kg/m^{2}s, the irreversible pressure drop for the corrugated surface is 36% higher than that for the smooth surface for the NARM. Note that the pressure drop of the NARM is approximately 25% less than the pressure drop of R-22 for both geometries at a given mass flux.

CONCLUSIONS AND RECOMMENDATIONS

The average measured heat transfer coefficient for both the commercially available smooth and corrugated tubes increased, as expected, with increasing mass flux for R-22 and the NARM. The average heat transfer coefficient for the corrugated tube geometry was typically 70% higher that for the smooth tube for the NARM and 40% higher than that for the smooth tube for R-22. Compared with the smooth tube, the corrugated tube geometry enhanced heat transfer for all mass fluxes.

The corrugations of the enhanced tube affect the heat transfer observed for the NARM. The heat transfer coefficient is only 20% lower in the corrugated tube as compared to 60% lower in the smooth tube geometry as compared with R-22. Hence, the corrugated tube geometry is apparently mitigating the NARM heat transfer degradation mechanisms. One possible reason for this

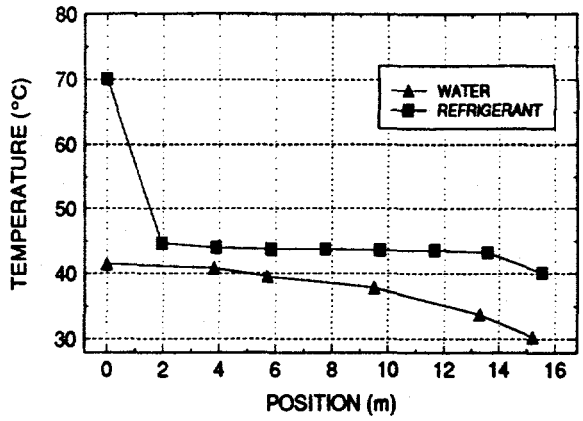

FIGURE 7. R-22 FLOWING INSIDE CORRUGATED TUBE AT MASS FLUX = 277 kg/m^{2}s .

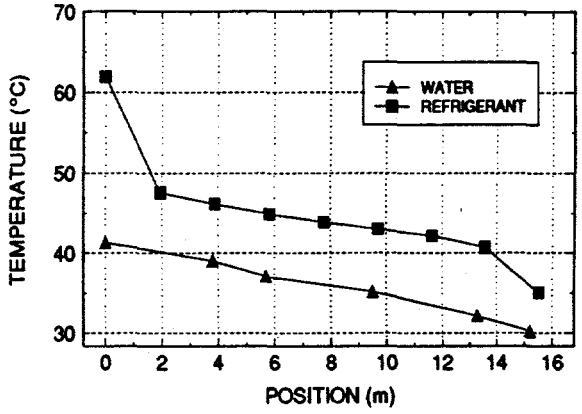

FIGURE 8. NARM FLOWING INSIDE CORRUGATED TUBE AT MASS FLUX = 495 kg/m^{2}s.

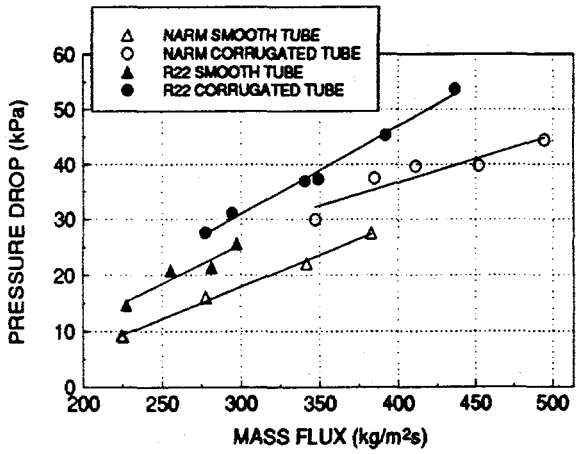

FIGURE 9. IRREVERSIBLE PRESSURE DROP FOR SMOOTH AND CORRUGATED TUBE CONDENSERS.

degradation mitigation is mixing of the constituent refrigerants due to the tube wall corrugated configuration. This enhancement in heat transfer, however, comes with an increase in pressure drop, also associated with the corrugations.

To characterize the heat transfer aspects of the corrugated tube, further investigation should consider the effect of the corrugated tube geometry—such as indentation height, pitch, and diameter—on the condensing characteristics of pure and mixed refrigerants.

ACKNOWLEDGMENTS

This research was sponsored by the U. S. Department of Energy, Office of Building Technologies, Building Equipment Division, under contract DE-AC05-84OR21400 with Martin Marietta Energy Systems, Inc. Dr. Hinton's participation was made possible by the U.S. Department of Energy's Historically Black Colleges and Universities Program through subcontract 19X-5B486V between Martin Marietta Energy Systems, Inc., and Tennessee State University.

REFERENCES

Box, G. E. P., Hunter, W. G., and Hunter, J. S., 1978, *Statistics for Experimenters*, John Wiley and Sons, New York, pp. 563–570.

Briggs, D. E. and Young, E. H., 1969, "Modified Wilson Plot Techniques for Obtaining Heat Transfer Correlations for Shell and Tube Heat Exchangers," *Chemical Engineering Progress, Symposium Series No. 92*, Vol. 65, pp. 35–45.

Granryd, E., and Conklin, J. C., 1990, "Thermal Performance Analysis for Heat Exchangers Using Nonazeotropic Refrigerant Mixtures," *Heat Transfer in Advanced Energy Systems*, R. F. Boehm and G. Vliet, eds., HTD-Vol. 151, AES-Vol. 18, The American Society of Mechanical Engineers, New York.

Miller, W. A., 1989, *Laboratory Study of the Dynamic Losses of a Single Speed, Split System Air-to-Air Heat Pump Having Tube and Plate Fin Heat Exchangers*, ORNL/CON-253, Oak Ridge National Laboratory, Martin Marietta Energy Systems, Inc., Oak Ridge, Tennessee.

Morrison, M., and McLinden, M. O., 1986, *Application of a Hard Sphere Equation of State to Refrigerants and Refrigerant Mixtures*, NBS-TN-1226, National Bureau of Standards, Gaithersburg, Maryland.

Rice, C. K., 1993, "Influence of Heat Exchanger Size and Augmentation on Performance Potential of Mixtures in Air-to-Air Heat Pumps," *ASHRAE Trans.*, Vol. 99, Part 2., pp. 665–679.

Schlager, L. M., Pate, M. B., and Bergles, A. E., 1990, "Performance Predictions of Refrigerant-Oil Mixtures in Smooth and Internally Finned Tubes—Part II: Design Equations," *ASHRAE Transactions*, Vol. 96, Pt. 1.

Shah, R. K., 1990, "Assessment of Modified Wilson Plot Techniques for Obtaining Heat Exchanger Design Data," *Heat Transfer 1990*, Vol. 5, Hemisphere, New York, pp. 51–56.

Vineyard, E. A., Conklin, J. C., and Brown, A. J., 1993, "Cycle Performance Testing of Nonazeotropic Refrigerant Mixtures of HFC-143a/HCFC-124 and HFC-32/HCFC-124 with Enhanced Surface Heat Exchangers,"*ASHRAE Trans.*, Vol.99(2).

Vineyard, E. A., Sand, J. R., and Statt, T. G., 1989, "Selection of Ozone-Safe, Nonazeotropic Refrigerant Mixtures for Capacity Modulation in Residential Heat Pumps," *ASHRAE Transactions*, Vol. 95, Pt. 1.